Research Article | Vol. 9, No. 2 | 1 Feb 2019 | OPTICAL MATERIALS EXPRESS 483
Optical Materials EXPRESS

Broadband saturable absorption and exciton-exciton annihilation in $MoSe_2$ composite thin films

GAOZHONG WANG,[1] AIDAN A. BAKER-MURRAY,[1] XIAOYAN ZHANG,[2,3] DANIEL BENNETT,[1,4] JING JING WANG,[1] JUN WANG,[2,3] KANGPENG WANG,[1,*] AND WERNER J. BLAU[1]

[1]*School of Physics and the Centre for Research on Adaptive Nanostructures and Nanodevices (CRANN), Trinity College Dublin, Dublin 2, Ireland*
[2]*Key Laboratory of Materials for High-Power Laser, Shanghai Institute of Optics and Fine Mechanics, Chinese Academy of Sciences, Shanghai 201800, China*
[3]*Laboratory of Micro-Nano Photonic and Optoelectronic Materials and Devices, Shanghai Institute of Optics and Fine Mechanics, Chinese Academy of Sciences, Shanghai 201800, China*
[4]*Theory of Condensed Matter, Cavendish Laboratory, University of Cambridge, J. J. Thomson Avenue, Cambridge CB3 0HE, United Kingdom*
**wangkangpeng@msn.com*

Abstract: Polyvinyl alcohol (PVA) was utilized as a matrix to host two-dimensional (2D) liquid-phase-exfoliated $MoSe_2$ nanosheets. These 2D $MoSe_2$/PVA composite thin films were experimentally proven to be preferable for efficient nonlinear optical devices. Our nonlinear optical study shows that these composite thin films possess strong saturable absorption (SA) over a wide wavelength range from 400 nm to 800 nm under the irradiation of femtosecond and nanosecond lasers. The SA property of our films was measured for various laser pulse durations, wavelength and linear absorption. Moreover, employing pump-probe, exciton-exciton annihilation was experimentally observed and studied at 800 nm. Our research gives clear insight into the photophysical properties of $MoSe_2$/PVA thin films and shows the material's potential as a photonic device.

1. Introduction

2D materials have been the focus of research in many fields due to their novel physical, chemical, optical, and mechanical properties. As a big branch of 2D materials, layered transition metal dichalcogenides (TMDs) such as MoS_2, $MoSe_2$, WS_2, WSe_2 and WSn_2 etc., are reported to possess improved optical performance, such as photoluminescence, when compared to their bulk counterparts [1–16]. Particularly, the nonlinear optical experiments indicate that 2D liquid-phase-exfoliated $MoSe_2$ has strong saturable absorption [17,18]. But the saturable absorption in 2D $MoSe_2$ has yet to be investigated systematically. Monolayer $MoSe_2$ was reported to possesses a uniform modulation depth of ~80 ± 3% and a saturation intensity of ~2.5 ± 0.4 MW/cm^2 excited by femtosecond lasers [17]. Few-laser $MoSe_2$ was measured to have different third-order NLO susceptibilities at different wavelengths [18]. It would be interesting to study and analyze how the NLO behavior of 2D $MoSe_2$ can be affected by irradiated laser pulses. Also, exciton dynamics has been independently reported in 2D $MoSe_2$ in room temperature [19,20]. Carrier kinetics plays an important role in a saturable absorber when it is utilized for passive mode-locking [13]. It is necessary to study the saturable absorber behavior and excited carrier dynamics simultaneously in 2D $MoSe_2$. The above questions indicate that there is still work to be done on the layered $MoSe_2$ in the field of nonlinear optics.

In this paper, a comparative study was performed to explore the relationship between the nonlinear optical behavior of $MoSe_2$/PVA composites and wavelength and, pulse duration.

#347092 https://doi.org/10.1364/OME.9.000483
Journal © 2019 Received 8 Oct 2018; revised 20 Nov 2018; accepted 14 Dec 2018; published 10 Jan 2019

Optical Materials EXPRESS

Liquid-phase exfoliation was employed to fabricate few-layer $MoSe_2$ nanosheets in water using sodium cholate as the surfactant. Polyvinyl alcohol powder was dissolved in warm water to prepare PVA solutions which were used as a host for $MoSe_2$/PVA composite thin films. By changing the concentration of $MoSe_2$ inside the PVA matrix, three composite thin films with different linear transmissions were fabricated. The nonlinear optical behavior of these composite thin films was investigated via open-aperture Z-scan techniques. Our results indicate that the $MoSe_2$/PVA thin films possess saturable absorption behavior in a wide wavelength region, 400 nm to 800 nm, under femtosecond and nanosecond pulses. This broadband saturable absorption shows an obvious dependence on both the linear absorption and irradiation laser wavelength. The nonlinear absorption, α_{NL}, and the third-order nonlinear optical susceptibility, $Im\chi^{(3)}$, are approximately three orders of magnitude larger under the irradiation of nanosecond pulses in comparison to femtosecond pulses. As the carrier relaxation processes are important when a saturable absorber is used for mode-locking in a pulses laser, a degenerate pump-probe technique was employed to study the excited carrier dynamics of our $MoSe_2$/PVA thin films. By studying the relationship between excitation carrier density and the pump-probe time, exciton-exciton annihilation was verified at a wavelength of 800 nm.

2. Materials and characterization

As a precursor to the fabrication of $MoSe_2$/PVA composite thin films, two dimensional $MoSe_2$ flakes were prepared from bulk $MoSe_2$ in the distilled (DI) water using sodium cholate (SC) as a surfactant using a liquid-phase exfoliation technique [14,15,21]. 1g $MoSe_2$ powder was dispersed in 20 ml aqueous surfactant solution with a concentration of SC of 10 mg/ml. The $MoSe_2$ mixture was first sonicated using a sonic tip for 90 min using a 40% amplitude with pulses of 2 s on and 4 s off. After sonication, monolayer, bilayer and few-layer $MoSe_2$ flakes were obtained from the bulk limit. The sonicated dispersion was then centrifuged at 2000 rpm for 90 mins to remove large flakes and bulk. A 2D $MoSe_2$ dispersion was finally obtained by collecting the top ½ of the centrifuged dispersion. The thickness distribution of 2D $MoSe_2$ flakes was studied using an atom force microscopy (AFM). Figure 1(a) shows a AFM image in a 4 μm × 4 μm area, in which stacked flakes can be seen. Except for these stacked flakes, the $MoSe_2$ dispersion was composed of few-layer flakes. As seen in Fig. 1(b), the flakes with layer number less than 15 account for ~88% of the dispersion.

To prepare PVA solutions, 0.5 g of PVA powder was dispersed into 10 ml of DI water, following by heating in a water bath on a stirring hot plate. After cooling down to room temperature, 10 ml of the resultant PVA solutions were mixed with 50 μl, 100 μl and 150 μl of $MoSe_2$ flake dispersions respectively. These mixtures were stirred for 12 hours using magnetic stir bars, then subsequently sonicated for 5 minutes at a low power to achieve homogeneous mixed solutions. These mixed solutions were cast into petri dishes and dried in an oven at 60 °C for 4 days. This produced 3 high-quality $MoSe_2$/PVA composite thin films, named α, β and γ from highest to lowest linear transmission, respectively, as shown in Figs. 1(d)-1(f). The thicknesses of α, β and γ were measured to be 202, 228 and 264 μm, respectively. Pure PVA films were also prepared using the same solution cast method to exclude the contribution of PVA to the nonlinear optical properties of the composite thin films. The ground state absorption spectra of these thin films are plotted in Fig. 1(c). An absorption peak can be seen clearly at 800 nm for all of the composite thin films while none are observed for the pure PVA film.

Optical Materials EXPRESS

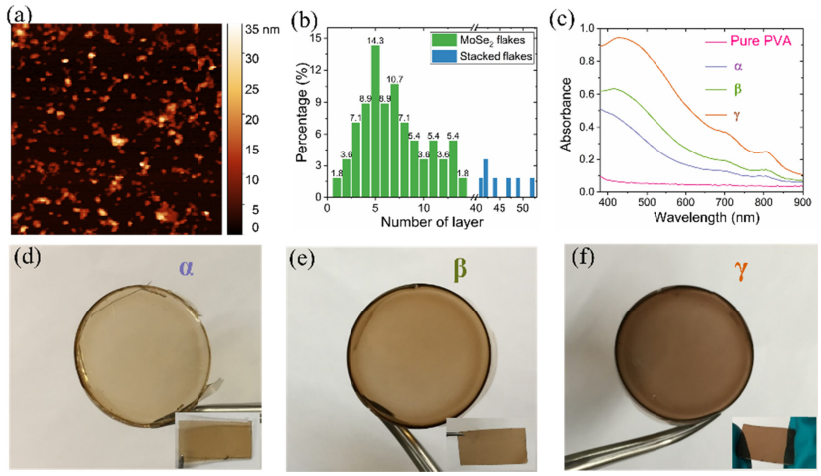

Fig. 1. (a) A AFM image consist of a large amount of $MoSe_2$ flakes for (b) thickness statistics in a 4 μm × 4 μm area. (c) The ground state absorption spectra of pure PVA and $MoSe_2$ composite thin films. (d)-(f). The photos of the three composite thin films (α, β and γ).

3. Saturable absorption of $MoSe_2$/PVA thin films

The optical nonlinear study of these thin films was then performed using open-aperture Z-scan techniques based on two laser regimes: firstly, a Q-switched Nd:YAG laser with 6 ns pulse duration, 10 Hz repetition rate and a wavelength of 532 nm, and secondly, a Ti:Sapphire amplifier (Coherent RegA 9000) with ~100 femtosecond pulse duration, 100 kHz repetition rate at the wavelengths of 400 nm, 500 nm and 800 nm. 400 nm and 500 nm ultrafast pulses were generated from a Coherent optical parametric amplifier (OPA 9800) that is driven by 800 nm pulses from the Ti:Sapphire laser.

3.1 Dependence of SA on pulse duration

Figures 2(a)-2(c) show the Z-scan results from the nanosecond laser at 532 nm while Figs. 2(e)-2(f) display the 550nm data from the femtosecond laser. The thin films at all examined wavelengths and pulse durations exhibit obvious saturable absorption, *i.e.*, the transmission of the composite thin films increase with incident laser intensity. To theoretically analyze these results, the nonlinear optical theory was utilized to model the experimental Z-scan traces. The propagation equation in $MoSe_2$/PVA thin films is $dI/dz = -\alpha(I)\cdot I$, where I represents the excitation laser intensity, z is the propagating distance in the composite thin film, and $\alpha(I)$ is the total absorption that consists of linear absorptive, α_0, and nonlinear absorptive coefficients, α_{NL}: $\alpha(I) = \alpha_0 + \alpha_{NL}\cdot I$. This propagation equation was used to fit the experimental results and gives good fits for all the wavelengths and pulse durations. The experimental results in the nonlinear optical figures are shown using points and the fits are shown using solid lines.

Optical Materials EXPRESS

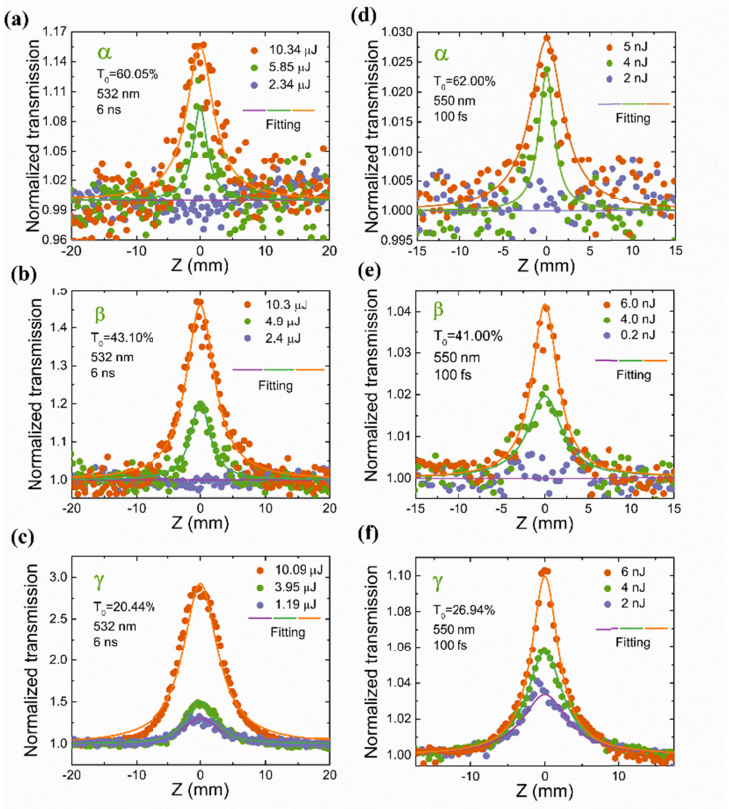

Fig. 2. The experimental and fitting results of $MoSe_2$/PVA thin films based on 6ns (10 Hz) and 100 fs (100 kHz) laser pulses at the center wavelength of 532 nm and 550 nm, respectively. The measurements were carried out on three composite thin films (α, β and γ) with different linear transmission using variable energies.

The fitted linear and nonlinear optical parameters of the composite thin films are listed in Table 1 for 532 nm, 6 ns laser pulses, and Table 2 for 550 nm, 100 fs laser pulses. Under irradiation of the laser with wavelength of 532 nm, pulse duration of 6 ns and repetition rate of 10 Hz, the linear transmission, T_0, of the composite thin films were measured to be 59.6%, 42.8% and 19.9% respectively. Based on these linear transmissions, the corresponding linear absorptions, α_0, were calculated to be 13.5 cm^{-1}, 25.0 cm^{-1} and 39.4 cm^{-1} respectively. As the linear absorption was changed from 13.5 cm^{-1} to 39.4 cm^{-1}, the nonlinear absorption changed from −26.1 cm/GW to −960.0 cm/GW. Thus, the $MoSe_2$/PVA composite thin films with lower linear absorption have smaller nonlinear absorption. This suggests that the saturable absorption increases with the increase of the content of $MoSe_2$ in the polymer host. This relationship between saturable absorption and linear absorption has also been observed in other 2D nanosheets such as graphene [22]. As one of the most important nonlinear optical parameters, the imaginary part of the third-order nonlinear optical susceptibility related to α_{NL} can be calculated by [22]:

$$\mathrm{Im}\,\chi^{(3)} = \left(\frac{10^{-7} c\lambda n^2}{96\pi^2}\right)\alpha_{NL} \qquad (1)$$

where c is the speed of light, λ is the irradiation wavelength and n is the refractive index. $\mathrm{Im}\chi^{(3)}$ was calculated to be -1.0×10^{-11} esu, -33.6×10^{-11} esu and -37.2×10^{-11} esu for α, β, and γ, respectively. Here, esu is the electrostatic units. It is clear that $\mathrm{Im}\chi^{(3)}$ increases with the

Optical Materials EXPRESS

linear absorption. This is consistent with the dependence of saturable absorption on the concentration of the nonlinear materials. The Figure of Merit (FOM) is defined as the $\mathrm{Im}\chi^{(3)}$ value per 1/cm to eliminate the discrepancy of different linear absorption:

$$FOM = \left| \frac{\mathrm{Im}\,\chi^{(3)}}{\alpha_0} \right| \tag{2}$$

The calculated parameters from Eq. (2) are also shown in Table 1. The calculated FOM values all have similar orders of magnitude.

Table 1. The fitting parameters of Z-scan results and optical nonlinearities of the composite thin films α, β and γ with linear transmission of 59.6%, 42.8% and 19.9% respectively at 532 nm. The pulse duration of the laser is 6 ns and the pulse repetition rate is 10 Hz.

Laser pulse	Sample	T_0 (%)	α_0 (1/cm)	Energy	ω_0 (μm)	NLO	α_{NL} (cm/GW)	Im χ (3) (× 10^{-13} esu)	FOM (× 10^{-14} esu cm)
532 nm 6 ns 10 Hz	α	59.6	13.5	2.34 μJ	-	-	-	-	-
				5.85 μJ	15.4	SA	–26.1	–101.4	75.3
				10.34	21.6	SA	–44.7	–173.6	128.8
	Averag			-			–35.4	–137.5	102.0
	β	42.8	24.9	2.4 μJ	-	-	-	-	-
				4.9 μJ	18.4	SA	–119.2	–462.6	185.5
				10.3 μJ	23.9	SA	–1612.6	–6257.0	2509.4
	Averag			-			–865.9	–3359.8	1347.5
	γ	19.9	39.4	1.19 μJ	25.7	SA	–1612.6	–6257.0	1588.7
				3.95 μJ	23.0	SA	–535.4	–2077.3	527.4
				10.09	34.3	SA	–732.0	–2840.4	721.2
	Averag			-			–960.0	–3724.9	945.8

Table 2. Linear and nonlinear optical parameters of the composite thin films based on a pulse laser with a center wavelength of 550 nm, pulses duration of ~100 fs and 100 kHz repetition rate. The linear transmission of the samples α, β, and γ at 550 nm are 61.9%, 41.0% and 26.9% respectively.

Laser pulse	Sample	T_0 (%)	α_0 (1/cm)	Energy	ω_0 (μm)	NLO	α_{NL} (cm/GW)	Im χ (3) (× 10^{-13} esu)	FOM (× 10^{-14} esu cm)
550 nm ~100 fs 100 KHz	α	61.9	12.8	2 nJ					
				4 nJ	13.6	SA	–0.1	–0.6	0.4
				5 nJ	20.2	SA	–0.3	–1.2	0.9
	Average						–0.2	–0.9	0.7
	β	41.0	25.9	2 nJ					
				4 nJ	20.6	SA	0.4	–1.5	0.6
				6 nJ	17.8	SA	0.4	–1.6	0.6
	Average						0.4	–1.6	0.6
	γ	26.9	36.2	2 nJ	25.8	SA	–2.3	–9.8	2.7
				4 nJ	23.1	SA	–1.6	–6.5	1.8
				6 nJ	20.2	SA	–1.3	–5.5	1.5
	Ave						–1.7	–7.2	2.0

For comparison, the wavelength of the femtosecond laser was tuned to 550 nm, the closest wavelength we could achieve. The linear and nonlinear parameters for this wavelength are listed in Table 2. FOM of all the thin films was calculated to be of the order of 10^{-15} esu cm.

Optical Materials EXPRESS

This is very closed to that in graphene/PVA, indicating the interesting NLO behavior in MoSe2/PVA thin films. The linear absorption at 550 nm was measured to be 12.8 cm^{-1}, 25.9 cm^{-1} and 36.2 cm^{-1} for samples α, β and γ, respectively, which are all slightly lower than at 532 nm, *i.e.*, 13.5 cm^{-1}, 25.0 cm^{-1} and 39.4 cm^{-1}. This agrees with the fact that $MoSe_2$ possesses higher linear absorption at shorter wavelengths [18]. It also shows the accuracy of the method to measure the linear absorption. Similar to the nanosecond laser, strong saturable absorption was also observed under the irradiation of the femtosecond laser. At the same time, the nonlinear parameters including α_{NL} and $\mathrm{Im}\chi^{(3)}$ rise with the level of $MoSe_2$ content in the host. This is consistent with the case for the nanosecond laser, shown Table 1. The values of α_{NL} were fitted to be –0.2 cm/GW, –0.4 cm/GW and –1.7 cm/GW, and the values of $\mathrm{Im}\chi^{(3)}$ were calculated to be -0.884×10^{-13} esu, -1.6×10^{-13} esu and -7.2×10^{-13} esu for samples α, β, and γ, respectively. Both α_{NL} and $\mathrm{Im}\chi^{(3)}$ for the femtosecond laser are two orders of magnitude lower than the values for the nanosecond laser. Similar results were also reported in graphene/PVA thin films. $\mathrm{Im}\chi^{(3)}$ of a graphene/PVA was measured to be $\sim 10^{-13}$ esu for 340 fs pulses 1030 nm and 10^{-11} esu for 6 ns pulses (1064 nm) [22].

This dependence of saturable absorption on the pulse duration can be explained by excited carrier dynamics. Few-layer $MoSe_2$ is an indirect bandgap semiconductor. The incident light injects excited carriers into the conduction and valence band. Initially these carriers are in a non-equilibrium state and will be a thermalized rapidly to a quasi-thermal state via carrier-carrier scattering in a very short time of ~10 - 200 fs. These quasi-thermal carriers are subsequently cooled down via intraband carrier-photon scattering at τ_r ~1.9 ps and finally these excited carriers are annihilated in τ_2 ~49.5 ps (see part 4). Hence, the recovery time (τ_r) of the excited carrier in the composite thin films can be approximated by $\tau_r = \tau_1 + \tau_2 \approx 52$ ps. It is obvious that the pulse duration (τ_p = 6 ns) of the nanosecond laser is much longer than the recovery time ($\tau_p >> \tau_r$). As a nonlinear material with saturable absorption property, the conduction band of $MoSe_2$ can be fully filled by the accumulation of the excited carrier and will no longer accept incoming carriers before relaxation. Consequently, the density of the excited carrier (N) can be approximately calculated by: $N = \alpha I \tau_r / h\upsilon$, while it should be expressed as: $N = \alpha I \tau_p / h\upsilon$ for a femtosecond laser whose pulse duration (τ_p = 100 fs) is much shorter than the recovery time of the composite thin films. For the same thin film, the density of the excited carrier at saturable state are always the same. Therefore, the saturable intensity (I_{sn}) for the nanosecond laser is smaller than for the femtosecond laser: $I_{sn} < I_{sf}$. According to equation $\alpha(I) = \alpha_0 + \alpha_{NL} \cdot I$ and $\alpha(I) = \alpha_0 / [1 + (I/I_s)]$, one can have $\alpha_0 + \alpha_{NL} \cdot I = \alpha(I) = \alpha_0 / [1 + (I/I_s)]$, where α_{NL} is negative. Hence, the nonlinear optical coefficient of the composite thin film obtained by the nanosecond laser is much larger than that the one obtained using the femtosecond laser.

Optical Materials EXPRESS

3.2 Broadband SA of $MoSe_2$/PVA thin films

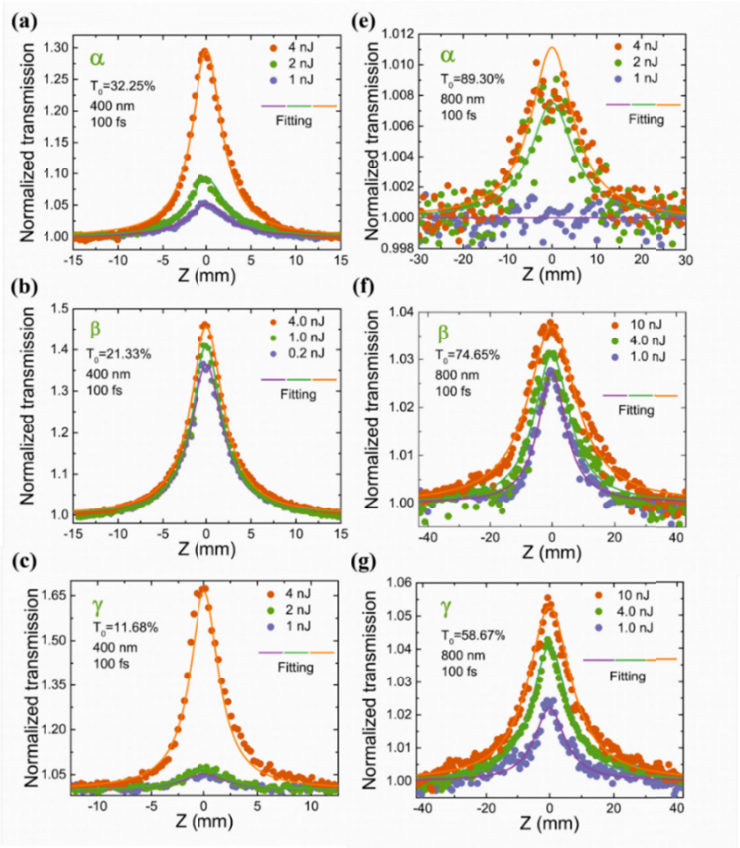

Fig. 3. The Z-scan results of $MoSe_2$/PVA thin films (α , β and γ) under femtosecond pulses laser radiation at the wavelengths of 400 nm and 800 nm.

The nonlinear optical response of the $MoSe_2$/PVA thin films at 400 nm and 800 nm were also studied, as seen Figs. 3(a)-3(c) and Figs. 3(e)-3(f), respectively. Saturable absorption was observed for the three samples at the both wavelengths. The fitting parameters from the propagation equation in nonlinear mediums for 400 nm and 800 nm are listed in Tables 3 and 4, respectively. α_{NL} for samples α, β, and γ at the wavelength of 400 nm were found to be −2.3 cm/GW, −35.6 cm/GW and −4.2 cm/GW, and $\mathrm{Im}\chi^{(3)}$ were calculated to be -2.9×10^{-13}esu, -45.5×10^{-13} esu and -5.3×10^{-13} esu respectively. We see that the nonlinear optical parameters for the β are an order of magnitude lager than those of α and γ. α_{NL} for β under the pulse energy of 0.2 nJ is −84.0 cm/GW, which is an order of magnitude greater than the α (−2.5 cm/GW) and γ (−3.7 cm/GW). This introduces a larger error to the average values. This is likely caused by experimental inaccuracy due to the very low transmission of the composite thin film at 400 nm. The linear transmission of the thin film β is 74.5% for 800 nm but as low as 21.0% for 400 nm. In contrast, the dependence of the optical nonlinearities of $MoSe_2$/PVA thin films on the $MoSe_2$ concentration is very clear at 800 nm where the linear transmission is relatively higher. At this wavelength, α_{NL} is −0.06 cm/GW, −0.98 cm/GW and −3.8 cm/GW and $\mathrm{Im}\chi^{(3)}$ is -0.4×10^{-13} esu, -6.1×10^{-13} esu and -23.8×10^{-13} esu for α , β and γ , respectively.

Optical Materials EXPRESS

Table 3. Linear and nonlinear optical parameters of the thin films α, β, and γ obtained from 100 fs pulse laser with a center wavelength of 400 nm and a duration of ~100 fs. The linear absorption of the samples α, β, and γ at 800 nm are 22.9 cm^{-1}, 34.5 cm^{-1} and 43.7 cm^{-1}, respectively.

Laser pulse	Sample	T_0 (%)	α_0 (1/cm)	E	ω_0 (μm)	NLO	α_{NL} (cm/GW)	Im $\chi^{(3)}$ (× 10^{-13} esu)	FOM (× 10^{-14} esu cm)
400 nm ~100 fs 100 kHz	α	32.2	22.9	1 nJ	18.9	SA	–2.5	–3.2	1.4
				2 nJ	18.5	SA	–2.1	–2.7	1.2
				4 nJ	17.7	SA	–2.4	–3.1	1.3
	Ave						–2.3	–3.0	1.3
	β	21.0	34.5	0.2 nJ	18.7	SA	–84.0	–107.4	31.2
				1 nJ	18.5	SA	–17.6	–22.5	6.5
				4 nJ	19.4	SA	–5.2	–6.6	1.9
	Ave						–35.6	–45.5	13.2
	γ	11.7	43.725	1 nJ	18.2	SA	–3.7	–4.8	1.1
				2 nJ	17.2	SA	–2.3	–2.9	0.7
				4 nJ	16.6	SA	–6.5	–8.3	1.9
	Ave						–4.2	–5.3	1.2

Table 4. Linear and nonlinear optical parameters of the thin films α, β, and γ at a wavelength of 800 nm.

Laser pulse	Sample	T_0 (%)	α_0 (1/cm)	E	ω_0 (μm)	NLO	α_{NL} (cm/GW)	Im $\chi^{(3)}$ (× 10^{-13} esu)	FOM (× 10^{-14} esu cm)
800 nm ~100 fs 100 k Hz	α	89.2	3.6	10 nJ	-	-	-	-	-
				20 nJ	38.3	SA	–0.06	–0.4	1.1
				30 nJ	38.3	SA	–0.06	–0.4	1.1
	Ave						–0.06	–0.4	1.1
	β	74.5	11.1	4 nJ	37.3	SA	–1.4	–9.1	8.2
				10 nJ	42.3	SA	–0.8	–5.3	4.7
				20 nJ	49.2	SA	–0.7	–4.2	3.8
	Ave						–1.0	–6.2	5.6
	γ	58.6	20.5	1 nJ	38.4	SA	–6.0	–38.0	18.6
				4 nJ	41.8	SA	–3.3	–20.7	10.1
				10 nJ	45.8	SA	–2.0	–12.7	6.2
	Ave						–3.8	–23.8	11.6

3.3 Dependence of SA on linear transmission and wavelength

From both Fig. 3(a)-3(c) and Fig. 3(e)-3(g), we can see that the maximum normalized transmission rises with the linear absorption for 400 nm and 800 nm, respectively. This is clear when the comparative Z-scan curves of samples α, β, and γ for the same experimental parameters are plotted together, as seen in Fig. 4. Figure 4(a) shows the Z-scan results of the three samples under the irradiation of 6 ns pulses at 532 nm and ~5 nJ. Larger saturable absorption exists in the composite thin films with higher linear absorption. This dependence of optical nonlinearity of the $MoSe_2$/PVA thin films on the $MoSe_2$ concentration is also true for the ~100 fs pulses at 400 nm, 550 nm and 800 nm, as shown in Figs. 4(c), 4(b) and 4(d), respectively. This is related to the wavelength-dependent saturable absorption. Under the radiation of 100 fs laser pulses with an energy of 4 nJ, the maximum normalized transmission for 400 nm, 550 nm and 800 nm are measured to be 1.662, 1.057 and 1.042, see Fig. 3(c), Fig. 2(f) and Fig. 3(g) respectively. The linear transmission of the thin film γ is 11.7%, 26.9% and

Optical Materials EXPRESS

58.6% at wavelengths of 400 nm, 550 nm and 800 nm, with a corresponding linear absorption of 43.7 cm^{-1}, 36.2 cm^{-1} and 20.5 cm^{-1}, respectively. Hence it is clear that the broadband saturable absorption of $MoSe_2$/PVA composite thin films can be tuned by changing the percentage of $MoSe_2$ in the polymer host.

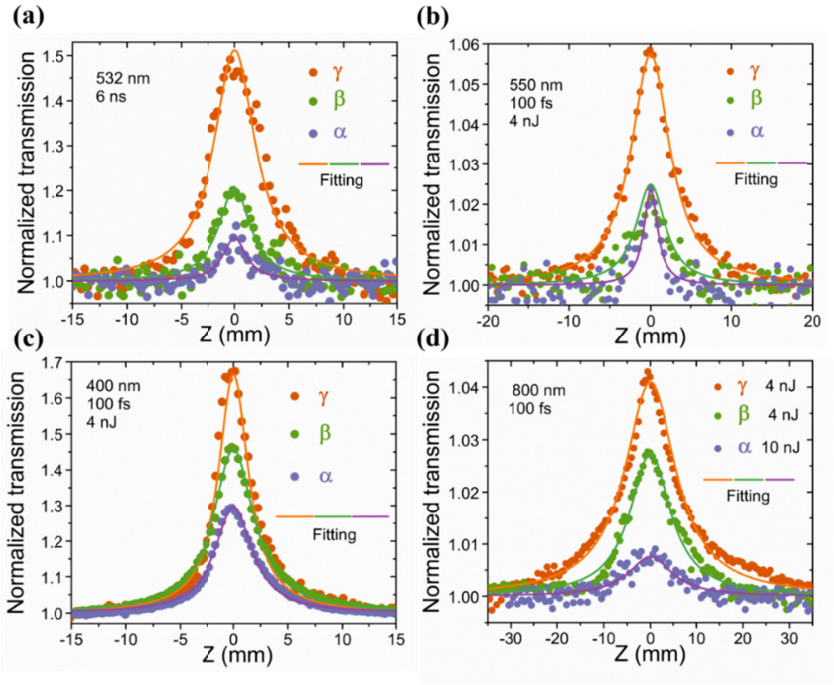

Fig. 4. (a) The Z-scan results of samples α, β, and γ under the irradiation of 6 ns pulses at 532 nm and ~5 nJ. The data for the ~100 fs pulses at the wavelength of (b) 550 nm, (c) 400 nm and (d) 800 nm.

4. Carrier dynamics of $MoSe_2$/PVA thin films

The excitation carrier dynamics play a significant role in the saturable absorber used in a mode-locking pulse laser. The carrier lifetime of the saturable absorber is a key factor to limit the pulse duration. In this section we study their excited carrier behaviors via degenerate pump-probe techniques. The schematic of the degenerate pump-probe set-up utilizes the ultrafast laser with a wavelength of 800 nm, pulse duration of ~100 fs and repetition rate of 100 kHz is plotted in Fig. 5(b). Both pump and probe beams were achieved from an 800 nm Ti:Sapphire femtosecond laser (Coherent RegA 9000). A beam splitter (~8/92) was employed to divide the initial 800 nm laser into two beams. The one with lower intensity was delayed by a motorized linear translation stage and then used for probing. The main beam was focused into the sample for pumping and was block by an aperture before the detector. An optical chopper was employed to modulate the pump and probe beams at 733 Hz and 422 Hz respectively.

Based on the above pump-probe set-up, the excitation carrier dynamics of two $MoSe_2$/PVA thin films (γ, $T_{0,\ 800\ nm}$ = 58.7%) were investigated at a wavelength of 800 nm, the pump energy fluence spanning from 10 nJ to 80 nJ in intervals of 10 nJ. Both pump and probe pulses were obtained from the same laser source and have a pulse duration of ~100 fs. Note that all the measurements were carried out at room temperature and under the damage threshold which guarantee the validity of the experimental results. Figure 5(a) plots the carrier dynamics traces for different pump energy fluences using solid scatters and circles with center dots of different colors. Photoinduced bleaching signal (*i.e.*, positive $\Delta T/T$) were

Optical Materials EXPRESS

observed for each pump energy fluence. The increase in the transmission at the early delayed time region right after excitation indicates that the saturable absorption of the composites thin films is due to Pauli-blocking. This agrees with the results of Z-scan.

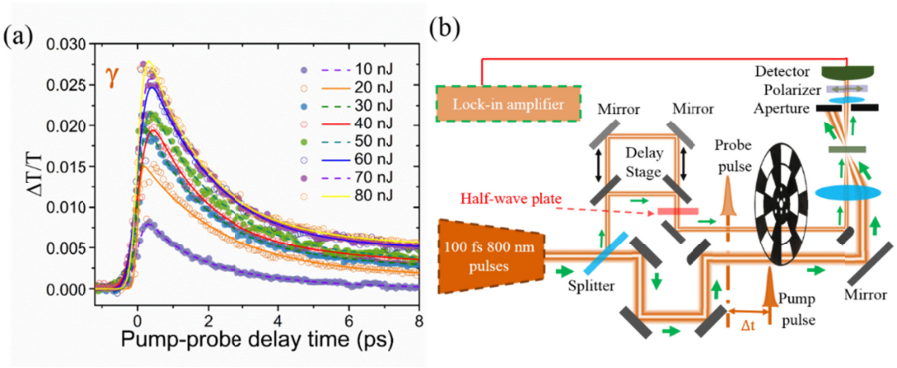

Fig. 5. (a) The differential transmission of $MoSe_2$/PVA thin films at different pump pulse energy obtained from (b) the degenerate pump-probe technique based on an 800 nm wavelength, ~100 fs and 100 kHz ultrafast laser.

From our experimental pump-probe data, we can easily see that for the excited carrier of $MoSe_2$/PVA there exists two exponential decay components with two characteristic carrier lifetimes. In order to determine the lifetime, a bi-exponential exponential decay model with autocorrelation was employed to model the carrier dynamics traces:

$$\Delta T/T = D_1 \exp\left(-\frac{t}{\tau_1}\right) erfc\left(\frac{\sigma}{\sqrt{2}\tau_1} - \frac{t}{\sqrt{2}\sigma}\right) + D_2 \exp\left(-\frac{t}{\tau_2}\right) erfc\left(\frac{\sigma}{\sqrt{2}\tau_2} - \frac{t}{\sqrt{2}\sigma}\right) \quad (3)$$

where τ_1 and τ_2 ($\tau_1 < \tau_2$) represent the short and the relatively long carrier lifetime, D_1 and D_2 are the corresponding relative amplitudes and σ is the fitting laser pulse duration. To obtain a desirable fit on the experimental data, a nonlinear least-squares algorithm was employed. The fitting parameters are listed in Table 5.

Table 5. The fitting parameters obtained from the bi-exponential decay equation used to model the pump-probe traces of $MoSe_2$/PVA.

Energy	D_1 (%)	D_2 (%)	τ_1 (ps)	τ_2 (ps)	σ (ps)
10 nJ	0.173	0.106	2.382	28.21	0.194
20 nJ	0.372	0.037	2.325	32.15	0.075
30 nJ	0.473	0.102	1.707	20.799	0.140
40 nJ	0.522	0.123	1.577	21.950	0.257
50 nJ	0.574	0.085	2.028	44.893	0.195
60 nJ	0.642	0.129	1.846	114.202	0.219
70 nJ	0.666	0.131	1.798	55.129	0.197
80 nJ	0.686	0.155	1.666	62.734	0.163
Average	0.513	0.108	1.916	47.508	0.180

The values of D_1 and D_2 at all the pump fluence energies are of the same order of magnitude with average values of 0.5% and 0.1%. This confirms the validity of the fittings. The average values of τ_1 and τ_2 were found to be 1.9 ps and 47.5 ps, respectively. It should be noted that neither the short time part nor the long-time part of the relaxation process gives obvious independence on the pump fluence.

Optical Materials EXPRESS

4.1 Exciton-exciton annihilation

Many studies on carrier dynamics have indicated that the relaxation rate of the excited carrier is helpful to understand the recombination mechanisms [19,23,24]. To develop a clear insight into the recombination processes, the recovery traces of the photoinduced carrier from excited states to the valence band are commonly described by a three-term rate equation [23–25]:

$$-dn/dt = An + Bn^2 + Cn^3 \tag{4}$$

where n is the excited carrier density and t is the relaxation time and A, B and C are constants. The first, second and third terms in the right-hand side of Eq. (4) represent first-order Shockley-Read-Hall (SRH) recombination, free-carrier recombination/exciton-exciton annihilation and Auger recombination, respectively [24,25]. By employing this rate equation to study the experimental data, one can determine the relaxation process of the excitation carrier.

An expression to describe the maximum differential transmission as a function of the initial excited carrier density can be written as [23,26]:

$$\left[\frac{\Delta T}{T}\right]_{\max} = \frac{\varepsilon n_0}{\gamma + n_0^{\eta}} \tag{5}$$

where $\varepsilon = -\delta A_{\max}/[\log(e)]$ and δ, γ and η are fitting parameters, and n0 is the initial excited carrier density. This expression leads to a relationship between $\Delta T/T$ and excited carrier density. The pump-probe traces in Fig. 5(a) shows that the maximum differential transmission increases continuously from ~0.8% to ~2.8% as the pump energy fluence increases from 10 nJ to 80 nJ. The pump energy fluence can be converted to pump photon fluence. As a result, the experimental $(\Delta T/T)_{\max}$ versus the initial photoinduced carrier density can be obtained, which is plotted in Fig. 6(a) using solid hexagons. By employing Eq. (5) to model the experimental data, the fitting parameters δ, γ and η can be obtained. The modelling result was plotted in Fig. 6. A close fit to the experimental results was obtained. Using the calculated values of δ, γ and η, the differential transmission as a function of excited carrier density at the pump-probe delay time, t, can be expressed as:

$$\frac{\Delta T}{T}(t) = \frac{\varepsilon n_t}{\zeta + n_t^{\eta}} \tag{6}$$

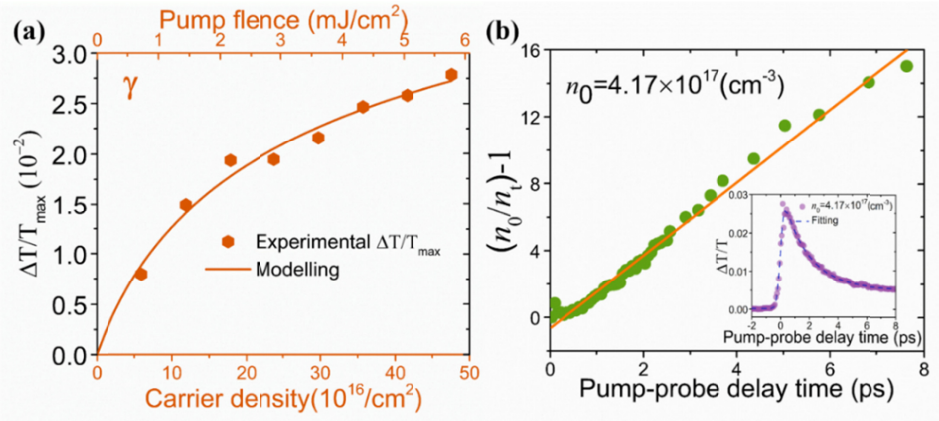

Fig. 6. (a) Maximum differential transmission as a function of initial photoinduced carrier density. (b) $(n_0/n_t - 1)$ as a function of the pump-probe delay time at initial photoinduced carrier density, n_0, of 4.17×10^{17} cm^{-3}. The inset is the corresponding carrier dynamics trace.

Optical Materials EXPRESS

Based on Eq. (6), one can convert the differential transmission at t to photoinduced carrier density, n_t, and hence obtain n_t as a function of t from the initial pump-probe traces. The inset of Fig. 6(b) shows a measured pump-probe trace of $MoSe_2$/PVA composite thin films with an excited photon density of 4.17×10^{17} cm^{-3}. Using Eq. (6) to transform the differential transmission to excited carrier density, the mechanism of recombination of excited carriers in $MoSe_2$/PVA can be investigated via the rate equation. To determine if it was dominated by second-order kinetics: $-dn/dt = \beta n^2$, was employed to analyze the data. By assuming the photoinduced electrons and holes are equivalent and integrating this equation, the rate equation to describe the second-order carrier dynamics is given by [19,23–25]:

$$\frac{n_0}{n_t} - 1 = \upsilon n_0 t \tag{7}$$

Here υ is the second-order recombination rate constant. The experimental n_0/n_t - 1 as a function of the pump-probe delay time at initial photoinduced carrier density of 4.17×10^{17} cm^{-3} is plotted in Fig. 6(b) using green solid circles. From the experimental data, $n_0/n_t - 1$ is proportional to the pump-probe delay time. This agrees with the rate equation of the second-order carrier dynamics. As no photoluminescence was observed from the few-layer samples, we exclude the free-carrier recombination. Consequently, this second-order recombination can be attributed to exciton-exciton annihilation. This is in agreement with the static exciton spectra as shown in Fig. 1(c). From linear fit from Eq. (5) to the converted excited carrier density, the exciton-exciton annihilation rate was obtained to be $(5.22 \pm 0.089) \times 10^{-6}$ cm^2/s, which is much slower than that in monolayer $MoSe_2$ (0.33 ± 0.06 cm^2/s) [19]. This could be attributed to the higher exciton density generated in monolayer than few-layer. In contrast, the rate in MoS_2 monolayer is much slower ($(4.3 \pm 1.1) \times 10^{-2}$ cm^2) and there is very little to report on the exciton-exciton annihilation in other few-layer materials in room temperature [25]. This indicates that 2D $MoSe_2$ has large potential applications in valleytronics.

5. Conclusion

In summary, a comparative study on the dependence of NLO properties of $MoSe_2$/PVA composites on laser wavelength, pulse duration, filler concentration, and linear absorption was carried out systematically. The NLO study was carried out using the open-aperture Z-scan technique with laser pulses with a 6 ns duration at the centeral wavelength of 532 nm and ~100 femtosecond laser pulses at the wavelengths of 400 nm, 500 nm and 800 nm. The $MoSe_2$/PVA thin films possess broadband saturable absorption behavior in a wavelength region from 400 nm to 800 nm under femtosecond, and nanosecond pulses. This saturable absorption is stronger in a composite thin film with higher linear absorption. Exciton-exciton annihilation was observed by the pump-probe study on the relationship between excitation carrier density and the pump-probe delay time at the wavelength of 800 nm, and their annihilation rate was obtained to be $(5.22 \pm 0.089) \times 10^{-6}$ cm^3/s.

Funding

Science Foundation Ireland (TIDA 207367).; NSFC (61675217 and 61522510); the Strategic Priority Research Program of CAS (XDB16030700); the Key Research Program of Frontier Science of CAS (QYZDB-SSW-JSC041); and the Program of Shanghai Academic Research Leader (no. 17XD1403900).

Acknowledgements

We are grateful for the discussions with Dr Brian Jennings and Dr Frank Bello.

Optical Materials EXPRESS

References

1. N. Dong, Y. Li, S. Zhang, X. Zhang, and J. Wang, "Optically Induced Transparency and Extinction in Dispersed MoS_2, $MoSe_2$, and Graphene Nanosheets," Adv. Opt. Mater. **5**(19), 1700543 (2017).
2. P. Tonndorf, R. Schmidt, P. Böttger, X. Zhang, J. Börner, A. Liebig, M. Albrecht, C. Kloc, O. Gordan, D. R. Zahn, S. Michaelis de Vasconcellos, and R. Bratschitsch, "Photoluminescence emission and Raman response of monolayer MoS□, MoSe□, and WSe□," Opt. Express **21**(4), 4908–4916 (2013).
3. D. H. Kim and D. Lim, "Optical second-harmonic generation in few-layer $MoSe_2$," J. Korean Phys. Soc. **66**(5), 816–820 (2015).
4. B. Liu, Y. Meng, X. Ruan, F. Wang, W. Liu, F. Song, X. Wang, J. Wu, L. He, R. Zhang, and Y. Xu, "Coupled relaxation channels of excitons in monolayer $MoSe_2$," Nanoscale **9**(46), 18546–18551 (2017).
5. Y. Zhang, T.-R. Chang, B. Zhou, Y.-T. Cui, H. Yan, Z. Liu, F. Schmitt, J. Lee, R. Moore, Y. Chen, H. Lin, H. T. Jeng, S. K. Mo, Z. Hussain, A. Bansil, and Z. X. Shen, "Direct observation of the transition from indirect to direct bandgap in atomically thin epitaxial $MoSe_2$," Nat. Nanotechnol. **9**(2), 111–115 (2013).
6. J. Koo, J. Park, J. Lee, Y. M. Jhon, and J. H. Lee, "Femtosecond harmonic mode-locking of a fiber laser at 3.27 GHz using a bulk-like, MoSe2-based saturable absorber," Opt. Express **24**(10), 10575–10589 (2016).
7. S. Horzum, H. Sahin, S. Cahangirov, P. Cudazzo, A. Rubio, T. Serin, and F. M. Peeters, "Phonon softening and direct to indirect band gap crossover in strained single-layer $MoSe_2$," Phys. Rev. B Condens. Matter Mater. Phys. **87**(12), 125415 (2013).
8. X. Zhang, A. Selkirk, S. Zhang, J. Huang, Y. Li, Y. Xie, N. Dong, Y. Cui, L. Zhang, and W. Blau, "Layered MoS_2 and carbon nanotube core-shell structured nanocomposites for enhanced nonlinear optical performances," Chemistry **23**, 3321–3327 (2017).
9. J. Lan, X. Zhang, Z. Zhou, B. Xu, H. Xu, Z. Cai, N. Chen, J. Wang, X. Xu, R. Soulard, and R. Moncorge, "Passively Q-Switched Tm: $CaYAlO_4$ Laser Using a MoS_2 Saturable Absorber," IEEE Photonics Technol. Lett. **29**(6), 515–518 (2017).
10. X. Zhang, S. Zhang, B. Chen, H. Wang, K. Wu, Y. Chen, J. Fan, S. Qi, X. Cui, L. Zhang, and J. Wang, "Direct synthesis of large-scale hierarchical MoS_2 films nanostructured with orthogonally oriented vertically and horizontally aligned layers," Nanoscale **8**(1), 431–439 (2016).
11. M. Shi, N. Dong, N. He, Y. Wan, H. Cheng, M. Han, J. Wang, and Y. Chen, "MoS_2 nanosheets covalently functionalized with polyacrylonitrile: synthesis and broadband laser protection performance," J. Mater. Chem. C Mater. Opt. Electron. Devices **5**(45), 11920–11926 (2017).
12. K. Wu, C. Guo, H. Wang, X. Zhang, J. Wang, and J. Chen, "All-optical phase shifter and switch near 1550nm using tungsten disulfide (WS_2) deposited tapered fiber," Opt. Express **25**(15), 17639–17649 (2017).
13. G. Wang, K. Wang, B. M. Szydłowska, A. A. Baker□Murray, J. J. Wang, Y. Feng, X. Zhang, J. Wang, and W. J. Blau, "Ultrafast Nonlinear Optical Properties of a Graphene Saturable Mirror in the 2 μm Wavelength Region," Laser Photonics Rev. **11**(5), 1700166 (2017).
14. G. Wang, S. Zhang, X. Zhang, L. Zhang, Y. Cheng, D. Fox, H. Zhang, J. N. Coleman, W. J. Blau, and J. Wang, "Tunable nonlinear refractive index of two-dimensional MoS_2, WS_2, and $MoSe_2$ nanosheet dispersions," Photon. Res. **3**(2), A51–A55 (2015).
15. G. Wang, G. Liang, A. A. Baker-Murray, K. Wang, J. J. Wang, X. Zhang, D. Bennett, J.-T. Luo, J. Wang, P. Fan, and W. J. Blau, "Nonlinear optical performance of few-layer molybdenum diselenide as a slow-saturable absorber," Photon. Res. **6**(7), 674–680 (2018).
16. A. Singh, G. Moody, S. Wu, Y. Wu, N. J. Ghimire, J. Yan, D. G. Mandrus, X. Xu, and X. Li, "Coherent electronic coupling in atomically thin $MoSe_2$," Phys. Rev. Lett. **112**(21), 216804 (2014).
17. Z. Nie, C. Trovatello, E. A. Pogna, S. Dal Conte, P. B. Miranda, E. Kelleher, C. Zhu, I. C. E. Turcu, Y. Xu, K. Liu, G. Cerullo, and F. Wang, "Broadband nonlinear optical response of monolayer $MoSe_2$ under ultrafast excitation," Appl. Phys. Lett. **112**(3), 031108 (2018).
18. K. Wang, Y. Feng, C. Chang, J. Zhan, C. Wang, Q. Zhao, J. N. Coleman, L. Zhang, W. J. Blau, and J. Wang, "Broadband ultrafast nonlinear absorption and nonlinear refraction of layered molybdenum dichalcogenide semiconductors," Nanoscale **6**(18), 10530–10535 (2014).
19. N. Kumar, Q. Cui, F. Ceballos, D. He, Y. Wang, and H. Zhao, "Exciton-exciton annihilation in $MoSe_2$ monolayers," Phys. Rev. B Condens. Matter Mater. Phys. **89**(12), 125427 (2014).
20. F. Gao, Y. Gong, M. Titze, R. Almeida, P. M. Ajayan, and H. Li, "Valley trion dynamics in monolayer $MoSe_2$," Phys. Rev. B **94**(24), 245413 (2016).
21. M. Lotya, Y. Hernandez, P. J. King, R. J. Smith, V. Nicolosi, L. S. Karlsson, F. M. Blighe, S. De, Z. Wang, I. T. McGovern, G. S. Duesberg, and J. N. Coleman, "Liquid phase production of graphene by exfoliation of graphite in surfactant/water solutions," J. Am. Chem. Soc. **131**(10), 3611–3620 (2009).
22. Y. Feng, N. Dong, G. Wang, Y. Li, S. Zhang, K. Wang, L. Zhang, W. J. Blau, and J. Wang, "Saturable absorption behavior of free-standing graphene polymer composite films over broad wavelength and time ranges," Opt. Express **23**(1), 559–569 (2015).
23. J. S. Manser and P. V. Kamat, "Band filling with free charge carriers in organometal halide perovskites," Nat. Photonics **8**(9), 737–743 (2014).
24. M. Ghanassi, M. Schanne□Klein, F. Hache, A. Ekimov, D. Ricard, and C. Flytzanis, "Time-resolved measurements of carrier recombination in experimental semiconductor□doped glasses: Confirmation of the role of Auger recombination," Appl. Phys. Lett. **62**(1), 78–80 (1993).

Optical Materials EXPRESS

25. D. Sun, Y. Rao, G. A. Reider, G. Chen, Y. You, L. Brézin, A. R. Harutyunyan, and T. F. Heinz, "Observation of rapid exciton-exciton annihilation in monolayer molybdenum disulfide," Nano Lett. **14**(10), 5625–5629 (2014).
26. I. Robel, B. A. Bunker, P. V. Kamat, and M. Kuno, "Exciton recombination dynamics in CdSe nanowires: bimolecular to three-carrier Auger kinetics," Nano Lett. **6**(7), 1344–1349 (2006).